Searching For Galaxy Clusters In The Dark Energy Survey

Adam Corness
School of Physics and Astronomy
University of Nottingham

17/05/2023

Abstract

Galaxy clusters are important objects for studying dark matter, dark energy, and the large scale structure of the universe. The aim of this project is to create a catalogue of candidate galaxy clusters in a $25\,\mathrm{deg}^2$ region of sky between $(73.5°, -58°)$ and $(75°, -56.5°)$ [format of (RA,DEC)]. The counts in cells algorithm was used on the I and Z band data from the Dark Energy Survey's Science Verification data release. First validating the algorithm functioned correctly on artificial imitations of galaxy clusters then on a known galaxy cluster - El Gordo. We identified 60 candidate galaxy clusters within the target area. When compared to a catalogue created by redMaPPer which identified 68 clusters in the same region of sky. We found 42% of identified candidate galaxy clusters were in close proximity (closer than $0.01125°$) to clusters identified by redMaPPer. The 60 candidate clusters displayed a red sequence on a (I-Z vs I band) colour magnitude diagram with a standard deviation on colour values of 0.36 which is 0.01 lower than the standard deviation of the colour across the whole field. The counts in cells algorithm suffered in precision when identifying clusters in regions with impurities such as cut out regions which are present across the DES SVA1 GOLD dataset. Counts in cells is also unable to discriminate between two galaxies at different depths due to no analysis of colour which may contaminate the resulting galaxy data with galaxies that are not in the cluster but are in front or behind it.

Contents

1 Introduction and Background

Galaxy clusters are the most massive objects in the universe. They typically contain hundreds of galaxies which are gravitationally bound. Because of their immense scale they create some of the most extreme environments of pressure, temperature and density in the universe. They contain large quantities of super hot x-ray emitting gas typically above 30 million Kelvin.[1] Galaxy clusters are predominantly composed of dark matter (approximately 80% by mass[2],) which makes them very good environments to study dark matter and its effects. Another significant use of galaxy clusters is studying the large scale structure of the universe which has many applications in developing cosmological models and studying dark energy.[3]

The objective of this project is to create create a set of candidate galaxy clusters from a region of the Dark Energy Survey's (DES) SVA1 GOLD catalogue[4], though this can be extended to other regions of the sky in the future. This catalogue could applied to gain a better understanding of dark matter and dark energy. The DES is a photometric survey of 1800deg^2 of the southern hemisphere, shown in figure 1. The most important information contained within the DES dataset for this project is a galaxies position and apparent brightness across multiple colour bands.

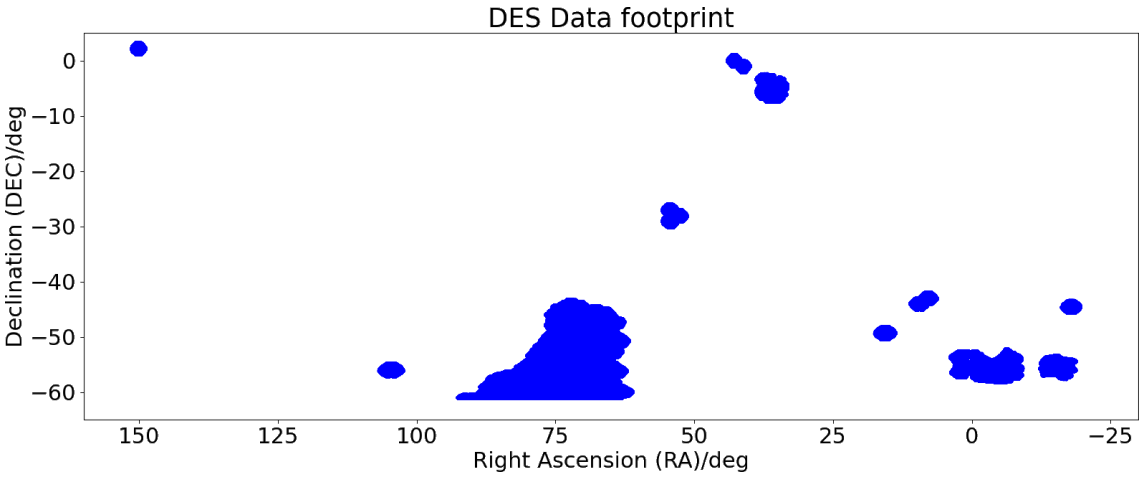

Figure 1: The footprint of the Dark energy survey. Each plotted pixel is a galaxy in the dataset. The resolution and scale of this plot is not sufficient to pick out individual galaxies but instead shows regions which the DES surveyed.

Early galaxy clusters were recorded in catalogues such as the Abell catalogue. Here clusters were identified by manually searching through survey printouts or photos.[5] Though a lot of time has passed since, the major improvements of galaxy cluster detection have been facilitated by advances in computing power, which allows clusters to be identified faster or with greater precision as new algorithms become computationally viable. The algorithm we chose to use for this project is counts in cells because the simplicity of implementation is appropriate for the scope of the project. The counts in cells algorithm divides the chosen field up into a set of cells and counts each galaxy that lies within a given cell. It then calculates a significance value for each cell which is a statistical quantification of the density of galaxies within a cell. A significance greater than 0 indicates that the galaxy has a higher density than an average cell in the field. Whilst the algorithm does not intrinsically use colour data, it can still be used to inspect the resulting candidate galaxy clusters to qualify if the precision of detection

is sufficient.

Galaxy clusters are predominantly composed from galaxies of similar age and will therefore be a similar colour. Because stars that are bright, hot, and blue have shorter lifespans, older galaxies will commonly appear redder than young galaxies due to these short lived stars dying out.[6] Additionally due to the effects of redshift, 3 identical galaxies will appear to have different colour if they are at different distances from us. These phenomena can be seen in a colour-magnitude diagram where members of a galaxy cluster will form a horizontal linear line known as a red sequence.[7]

The redshift of a galaxy cluster can be related to its angular size. This is described by the following equation:[8]

$$D_A = \left[\frac{c}{H_0}\int_0^z \left\{\Omega_M \left(1+z'\right)^3 + \Omega_k \left(1+z'\right)^2 + \Omega_\Lambda\right\}^{\frac{1}{2}} dz'\right]\left[1+z'\right]^{-1} \tag{1}$$

D_H is the angular diameter distance, it describes the ratio of an object's size to its angular size. Ω_M,Ω_k,Ω_Λ,c and H_0 are all cosmological constants that can be taken from Plank 2018 results[9]. Galaxy clusters have a characteristic size on the order of 1Mpc which means we can convert from angular diameter distance to angular size. Using this information and numerically solving equation 1 to give the following plots:

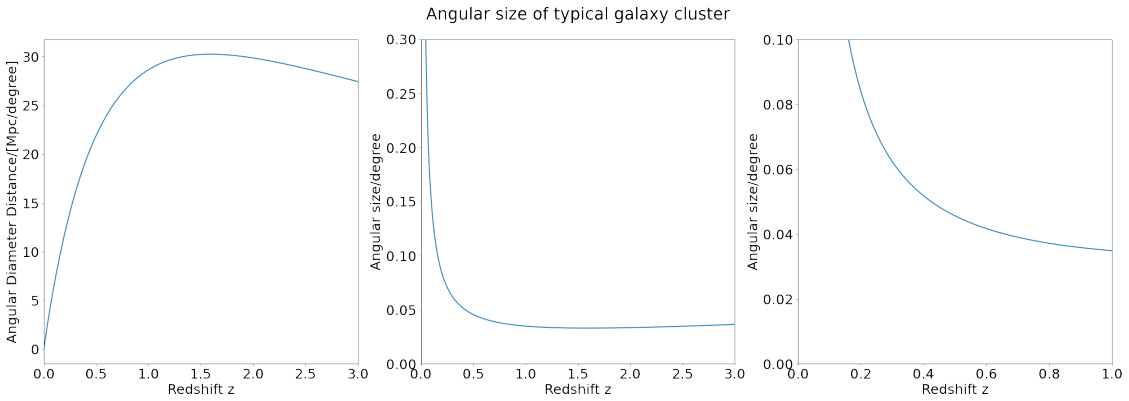

Figure 2: Left: A plot of $D_A(z)$ from equation 1. Note how the graph turns over at $z \approx 1.5$. Middle: A plot of $\frac{1}{D_A}$, the inverse of the left plot. As galaxy clusters have a characteristic size on the order of 1Mpc this can be used to directly convert angular size to redshift. Right: A cropped version of the middle plot to limit the range of redshifts used to a range appropriate for the DES dataset.

The counts in cells algorithm is sensitive to a galaxy clusters size and therefore the plots in figure 2 can be used to convert a cell size to a redshift to provide a rough estimate of a galaxy clusters redshift. The right plot in figure 2 shows the range of redshifts we will be capable of measuring using the DES SVA1 GOLD dataset, a majority of galaxy clusters we can detect will be within the range of z=0.2 to z=1.0.

2 Method

We used Python to implement the counts in cells algorithm. The first step was importing the DES dataset where we used the astropy and numpy Python modules to handle the .fits files containing the data. After selecting the columns of data we needed we exported the resulting array into a .npy file to make reading it into other Python files simple. Our implementation of

the counts in cells algorithm involved translating the data such that the minimum RA and DEC form x=0 and y=0. Then each point's new position elements were divided by the specified cell width and rounded down to the nearest integer, which gave the corresponding cell position. Then the count number of that cell was increased by 1. This was repeated for all points in the supplied dataset.

After all the points were counted, the following equation was used to calculate the significance of each cell[10]:

$$\sigma_{cl} = \frac{N_{cluster} - N_{field}}{\sigma_{field}} \tag{2}$$

Where $N_{cluster}$ is the number of points in the cell corresponding to the cluster, N_{field} is the mean number of points across all cells, σ_{field} is the standard deviation of N_{field}, and σ_{cl} is the significance of the cell corresponding to a cluster. It is a statistical measure of whether the cell contains an over density or under density. Candidate clusters can then be selected where a cell's significance is greater than a given value. This algorithm only requires positional information which made creating the algorithm in code straightforward.

Before applying counts in cells to the real DES dataset we generated sample sets. We did this creating a set of random points on a unit square to create a background signal. Then we added higher intensity Gaussian signals on-top of it with varying grouping tightness to simulate galaxy clusters at different redshifts:

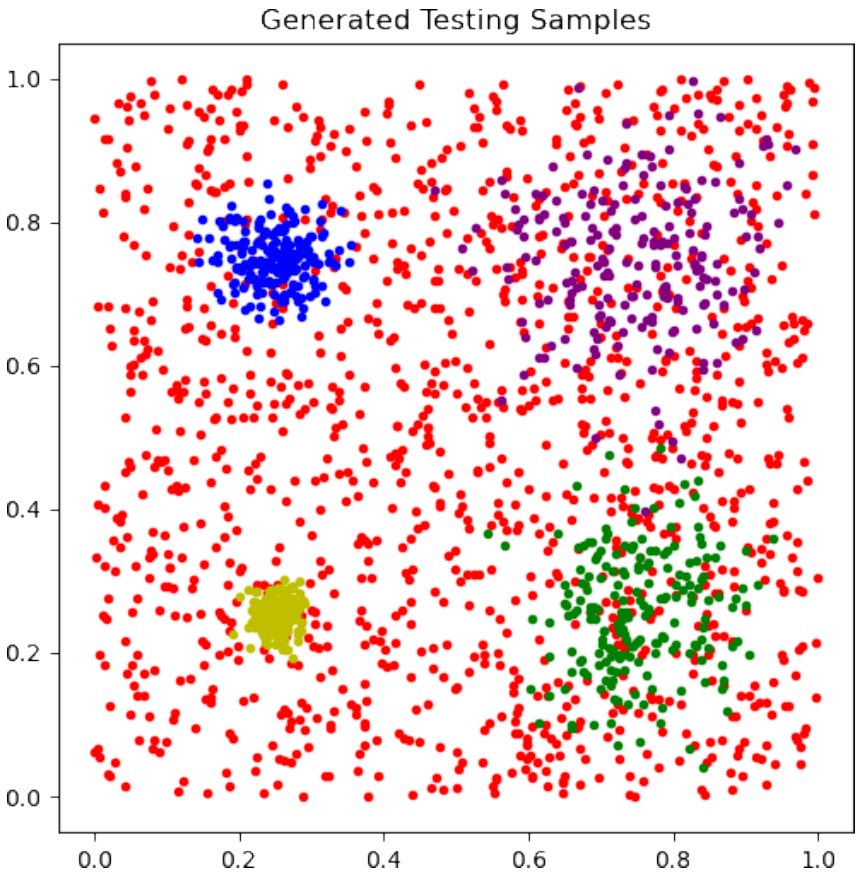

Figure 3: Plot of Gaussian test sources with equal number of points but varying spreads. Standard deviations from top left clockwise: $\sigma = 0.04$,$\sigma = 0.12$,$\sigma = 0.1$,$\sigma = 0.02$
Red points are the background signal whilst each other colour is a unique source. The x and y axes are in arbitrary units.

Figure 3 should act as a approximate model for galaxy clusters as each source has similar populations mimicking a galaxy cluster. Clusters will appear more compact when further, and more open when closer to an observer. Further clusters may appear with fewer galaxies however due to some galaxies being too dim to detect, though we attempted to mitigate this effect by eliminating galaxies dimmer than the magnitude turnover point.

When we ran the counts in cells algorithm on this generated sample we got these results for candidate clusters:

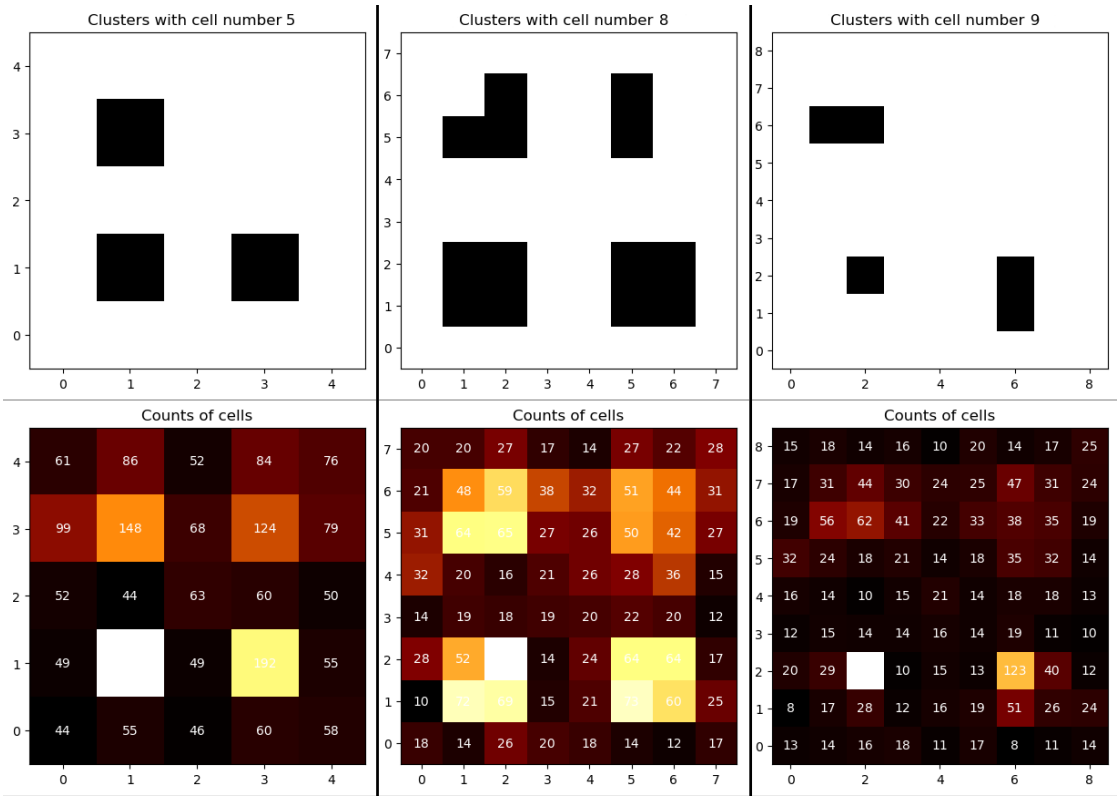

Figure 4: Graphs of candidate clusters and their corresponding counts in cells for varying cell sizes (left to right: 0.200, 0.125, 0.111). Top row is the identified candidate galaxy clusters with a significance threshold of 1 shown in black, whilst the lower row shows the number of points in each cell, brighter cells have more points within them. The x and y axes show the cell position and are in arbitrary units.

In figure 4 a significance threshold of 1 is used to qualify candidate clusters. This is because the generated sample has a high field standard deviation (σ_{field} from equation 2) due to the close proximity of dense signals, and will therefore lower each individual cell's significance. Figure 4 clearly shows that the algorithm is able to detect over densities. An interesting feature from figure 4 is how cell sizes impact cluster detection. The top right cluster is only detected at certain cell sizes. This is one of the major flaws with the counts in cells algorithm as cluster detection is impacted by galaxy clusters being pseudo-randomly divided across many cells, which will lower the cell significances compared to if the cluster was in a single cell. Whilst it is possible to remedy this for a single known galaxy cluster by translating the field area it's far more complex to do this systematically for a region of sky with unknown clusters.

After verifying the program was able to identify over densities, we then applied it to known objects from the DES dataset. DES includes a type flag on each object indicating if its a galaxy, star or unknown and a quality flag for if the object is blended or has bright neighbours that are partially obscuring it. When importing the dataset we only kept objects that were labelled both as galaxies and having no flags that indicated poor quality.

Additionally we plotted number magnitude histograms to identify where the turnover point of the data is. The turnover point is significant as it indicates where the data is incomplete. There are far more dim objects than bright ones so with perfect information collection you would expect an indefinite growth of objects at higher magnitudes. Real data collection methods have a finite resolving power, therefore dimmer objects will not all be detected.

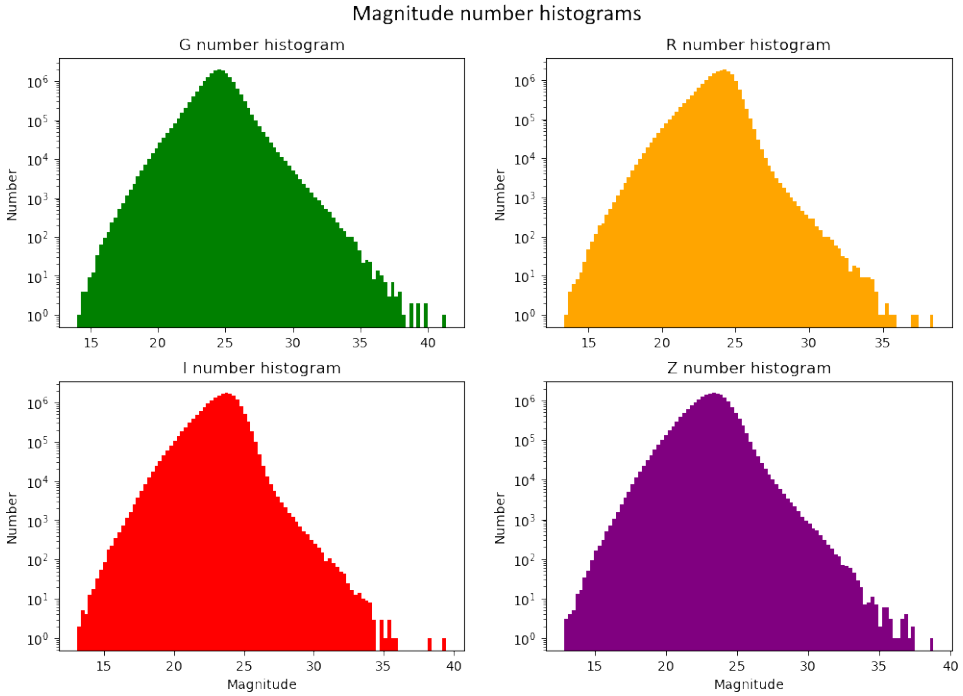

Figure 5: Magnitude histogram plots of all galaxies with no poor quality flags from the DES dataset in G,R,I, and Z filters. Each bands turnover point is around 25 mag.

The turnover point of the number magnitude histogram is a good indication of when the magnitude the data starts to become incomplete. We used figure 5 to determine the magnitude of the turnover point so we could then discard data that had higher magnitudes than this such that the remaining data was complete. We used the I band data which had a turnover point at 23.7 ± 0.2 mag. We used this to remove all points from our dataset with I band magnitudes over 23.7 mag. Figure 1 and figures from figure 6 and after were plotted using this contracted dataset.

We then plotted a footprint of the El Gordo cluster - a smaller isolated region of the DES with the cluster centered within it. Located approximately at $15°$ RA and $-49°$ DEC shown in figure 1. This provided a good sample to test the algorithm on real data. From the footprint plot of this area there were regions of data cut out or missing and edges to the area. Using the whole El Gordo region to calculate the field standard deviation would cause it to be far higher than the true value, this would lower every cells significance. To counteract this we took a small region nearby the El Gordo cluster devoid of any regions with missing data and used this to calculate the field standard deviation and mean (σ_{field} and N_{field} from equation 2). We used a significance threshold of 5 and a cell size of 0.075^2deg^2 to pick out just the El Gordo cluster but lower significance thresholds also found galaxy clusters in the surrounding region. We then plotted a colour magnitude diagram of the El Gordo cluster with I-Z bands on the y axis and I band on the x axis, and a pseudo-random non-candidate cell to see the red

sequence in the El Gordo cluster and compare it to the non cluster cell. The non-candidate cell was picked from the wider El Gordo region to be a good representation of an average cell in the field.

Once we were able to detect the El Gordo cluster we moved onto a region of the sky between 71° and 76°RA, and -60° to -55°DEC (SPT-E region). We also used a smaller region within this between 73.5° to 75°RA and -56.84° to -55.34°DEC to calculate the field standard deviation and mean in an identical fashion to the process in the El Gordo region. We used a significance threshold of 3 and a cell size of 0.075^2deg^2 to identify candidate clusters. Three is the lowest value the significance threshold can take whilst still producing statistically significant results. We then imported candidate galaxy clusters from redMaPPer, a more sophisticated detection algorithm,[11] so that we could compare our candidate clusters to candidate clusters in literature. We did this by classifying any of our candidate clusters that contained a redMaPPer cluster within its own cell and its 8 adjacent cells as a matched candidate. (This is equivalent to a square of area $0.1125^2\,\mathrm{deg}^2$ centered on candidate clusters.) We additionally plotted another colour magnitude diagram (again using I-Z vs I bands,) of the candidate clusters identified to verify that there weren't any candidates that had especially erroneous colour magnitude patterns. Though because far more clusters were present it is difficult to do this for each individual cluster.

3 Results

From figure 5 we determined the turnover points for each colour band: G :24.6 ± 0.2mag, R:24.1 ± 0.2mag, I:23.7 ± 0.2mag, Z:23.3 ± 0.2mag. We used the data from when we removed all points with I magnitude greater than 23.7 from the dataset, as the resulting array had the most points within it, when compared to repeating this process with the 3 other colour bands.

The footprint plot of the El Gordo Cluster region looked like this:

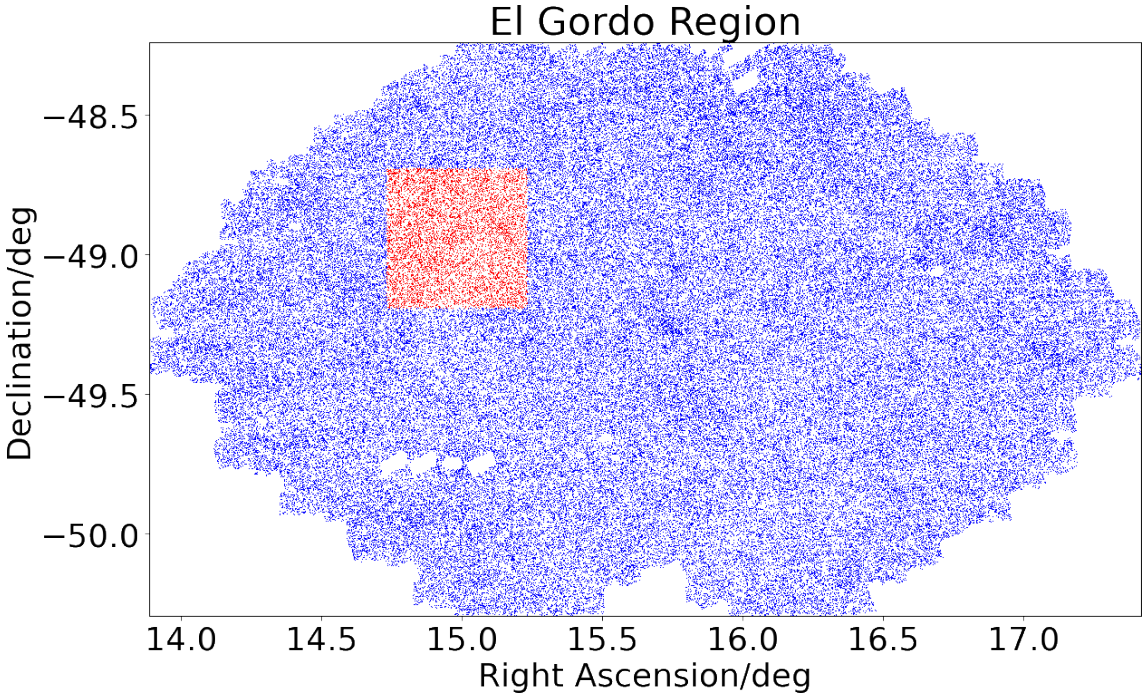

Figure 6: A footprint plot of the El Gordo cluster region. The red region is the area we used to calculate the field standard deviation and mean to be used in figure 7.

Figure 6 shows the region surrounding the El Gordo cluster. It is essentially a cropped version of figure 1. Some of the impurities in the dataset are clearly visible in figure 6 which were not visible in the footprint plot of the entire DES dataset. The main features that would impact the searching algorithm are the empty corners and the sequence of 4 voids in the lower left region of figure 6. There are also many smaller voids that are spread throughout the footprint plot. These are likely caused by bright neighbours and blended objects that we removed from the DES dataset. The red region within figure 6 is the region we used to calculate the field standard deviation and mean as it was free of any voids. The El Gordo cluster can be clearly seen in the center of the plot where the significant over density is The results of running the counts in cells algorithm on the El Gordo region are shown below:

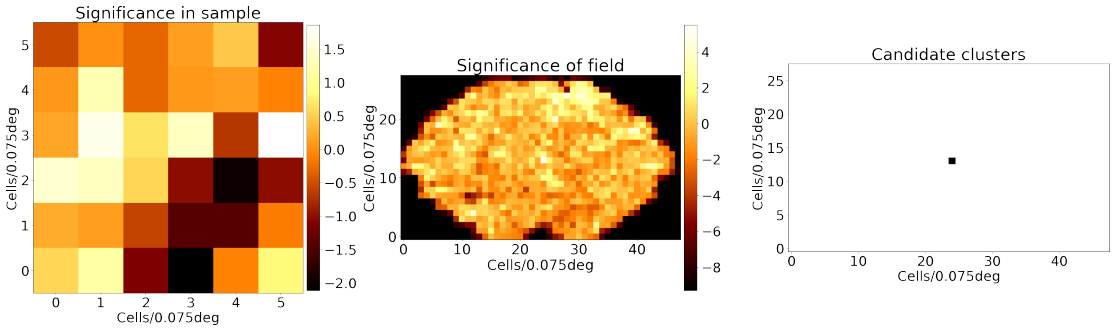

Figure 7: Counts in cells algorithm run on the El Gordo region with cellsize $= 0.075\text{deg}^2$ Left: Counts in cells algorithm run on the uniform region shown in red in figure 6 with resulting cell significance's shown. Middle: Counts in cells run on the wider El Gordo region using the field standard deviation and mean from the left plot as the field standard deviation and mean for the whole El Gordo region. The colour of a cell indicates its significance. Right: Cells from middle plot identified as candidate clusters where a cells significance was greater than 5 are shown in black.

In figure 7 we decided to use a high significance as it clearly picks out the El Gordo Cluster. The El Gordo cluster lies at a high redshift (z=0.87)[12], which is likely towards the higher limit of depth we will be able to identify galaxy clusters at. From figure 2 we can see that a redshift of 0.87 corresponds to an angular size of approximately $0.035°$ whilst an angular size of $0.075°$ corresponds to a redshift of z=0.25. This indicates that using a cell size of $0.075^2\,\text{deg}^2$ is a good compromise for the depth of the survey we are working with as it can identify galaxy clusters over a broad range of redshifts. This also gives us an upper and lower limit for the redshifts we are able to identify galaxy clusters at with this cell size - z=0.25 to z =0.87. From the identified candidate cluster cell we were able to extract the galaxies that lie within it

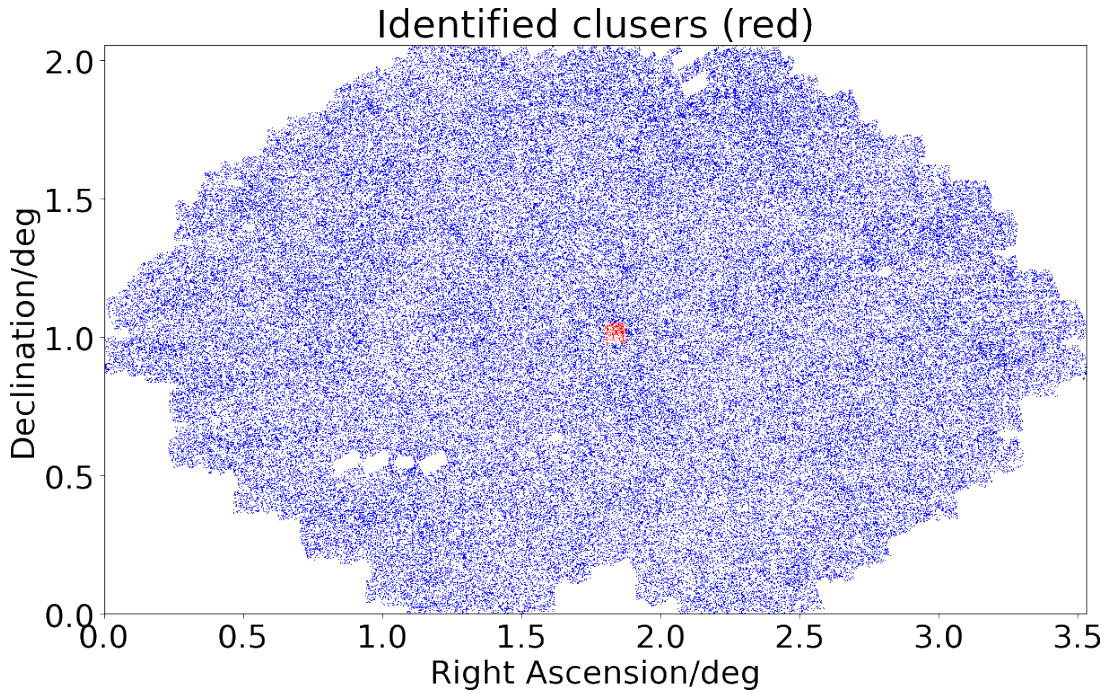

Figure 8: Footprint plot of El Gordo with galaxies that make up the candidate cluster cells shown in red. Note: this is translated to the origin, so whilst the x and y axis are accurately scaled they are not representative of where the region exists in the sky.

Whilst in figure 8 it appears the El Gordo cluster is not within a single cell it is still identified even at a high significance threshold of 5. This is likely because the El Gordo cluster is an atypically large galaxy cluster, and contains enough galaxies to be classified as a cluster despite the cell structure being misaligned from keeping the majority of the cluster within a single cell. Using the galaxy data from figure 8 we plotted a colour magnitude diagram for colour bands I-Z vs I of a non candidate cell manually selected to have a medium amount of galaxies within it, and a colour magnitude diagram of colour bands I-Z vs I of the identified candidate cluster cell.

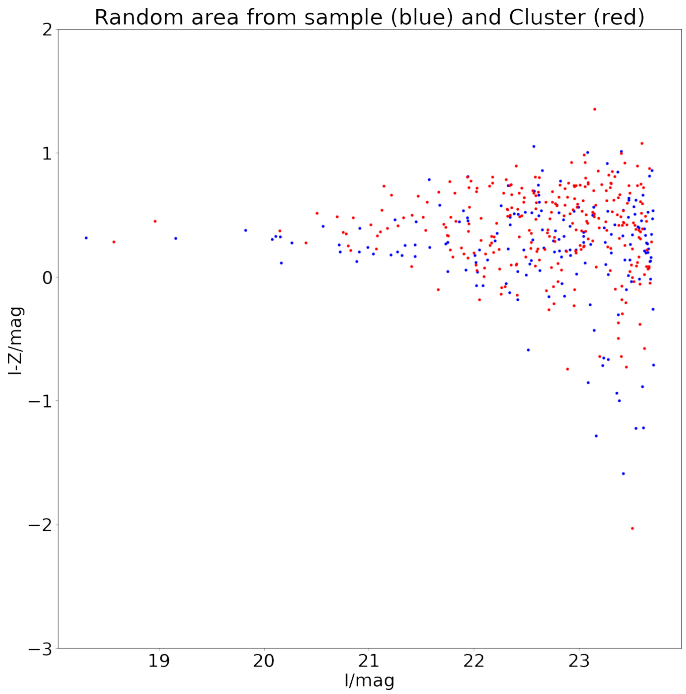

Figure 9: Colour magnitude plot of galaxies contained within candidate cluster cells (red), and of galaxies contained within a typical cell (blue).

At first glace it may appear that the red sequence is not present in figure 9. This is likely because the El Gordo cluster is a distant galaxy cluster which means it will appear dimmer than close galaxy clusters. Dimmer objects will have higher uncertainties on their magnitude measurements which is why the spread of the colour magnitude diagram increases with increasing magnitude and why the spread of the El Gordo cluster's colour is high. The standard deviation of the colour of the candidate cluster cell is 0.36 whereas the standard deviation of the normal cell's colour is 0.43 which is similar to the standard deviation of colour for the whole field - 0.46. Additionally the cluster cell has far more galaxies within it than the normal cell, 272 for the cluster and 171 for the normal cell. All these factors imply that the candidate cluster cell has selected a cluster and therefore the cluster identification algorithm has operated correctly.

Because we validated that the algorithm works on known clusters we moved onto a larger region of sky, within the SPT-E region of the DES dataset:

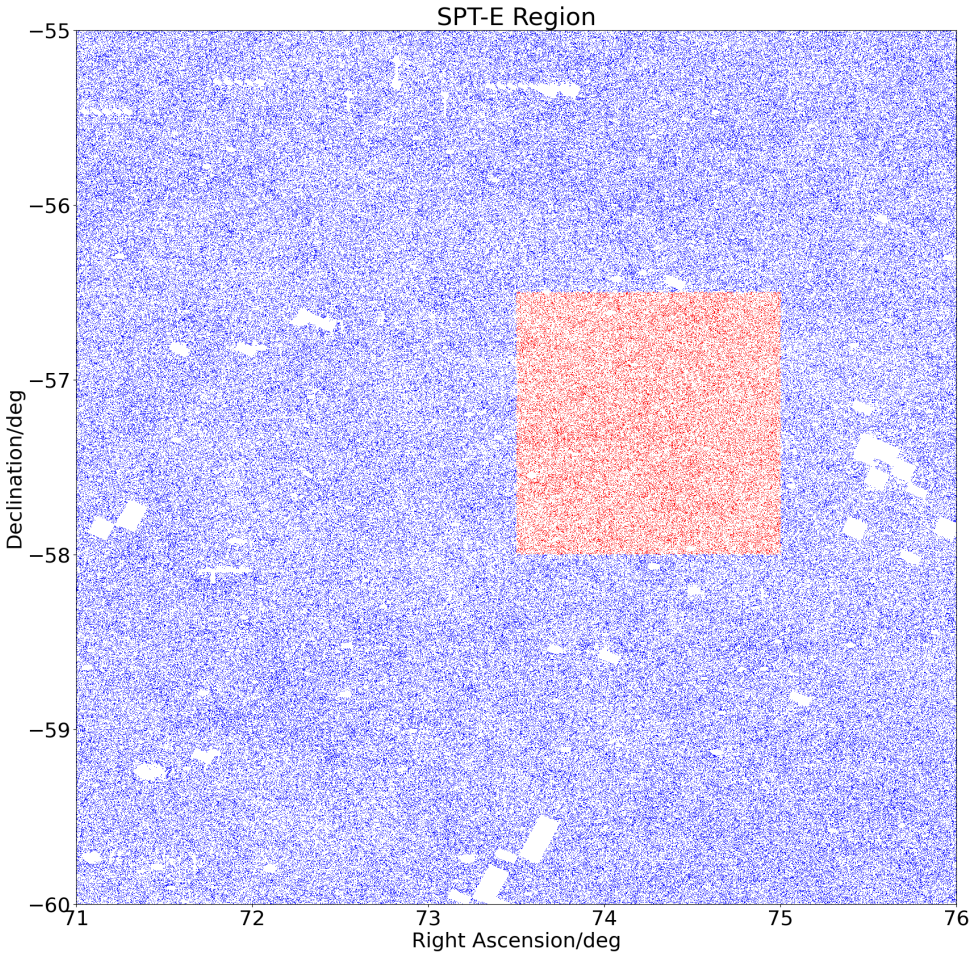

Figure 10: A footprint plot of a region of $25\,\mathrm{deg}^2$ centered at $73.5°$ RA, $-57.5°$ DEC. Points in red are in a region with minimal voids which was used to calculate the field standard deviation and mean.

The region in figure 10 is approximately 3 times larger than the El Gordo region in figure 6. It is apparent by visual inspection of figure 10 that there are significant over densities especially in the bottom left and top middle regions of the field. There also appears to be a higher density of voids in this region than the El Gordo region. Thankfully there was also a large region devoid of these cut out areas. Including one which is $1.5^2\,\mathrm{deg}^2$ that we decided to use for the calculation of field standard deviation and mean.

These are the results of running the counts in cells algorithm of the wider region in figure 6:

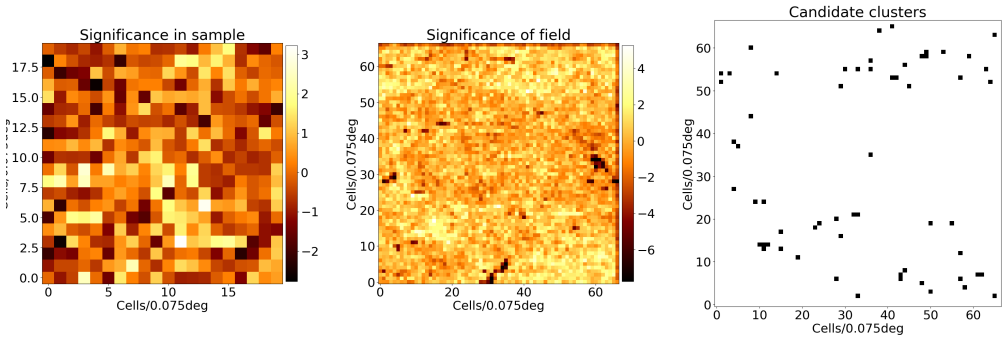

Figure 11: The 3 stages of the counts in cells algorithm working on figure 10. Left: Significance of cells corresponding to the red "clean" region in figure 10, used to calculate σ_{field} and N_{field}. Colour scale indicates significance of a cell. Middle: Significance of each cell in the whole field indicated by the colour scale. Right: Cells from the middle panel which have a significance greater than 3 are shown in black.

We used a cell size of $0.075^2\,\mathrm{deg}^2$ and a significance threshold of 3. This may produce some false positives given the significance threshold is low. The border of the middle plot shows a notably lower significance along the top and right side edges. This is because the size of the field does not divide evenly into full cells leaving these edge cells half full of data. This does not impact the rest of the field because of the way we calculated the field standard deviation and mean. The voids within the field are clearly visible in the central plot of figure 11, because of how the field was divided into cells the voids will mute the detection of galaxy clusters in the areas in the immediate vicinity of these voids.

This is how the candidate clusters in the right plot of figure 11 appear on the rest of the region:

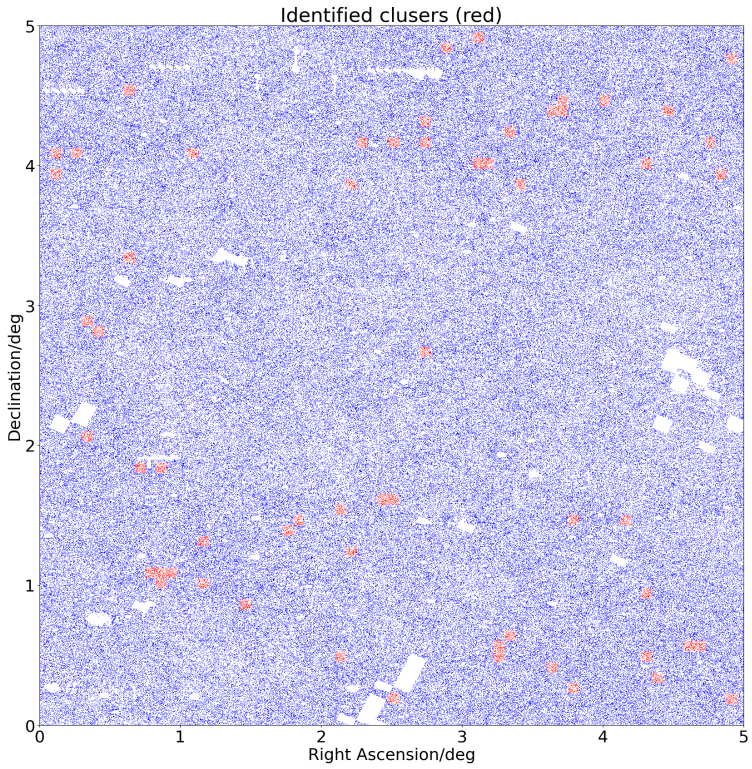

Figure 12: A plot of galaxies within candidate cluster cells in red on-top of the footprint plot of the SPT-E region in blue. Note: this is translated to the origin, so whilst the x and y axis are accurately scaled they are not representative of where the region exists in the sky.

One notable feature of figures 11 and 12 is a lack of detected clusters in the center of the field. This is likely a physical phenomena opposed to a fault with the detection algorithm or survey data, it may have an impact on the number of galaxies detected as the clean region we used was in this area of low cluster density, which may lower the field standard deviation and mean calculated. If the region was complete and didn't have missing sections; the field standard deviation of the whole section would be higher, and therefore less candidate clusters would be detected. In total we detected 60 candidate clusters.

We also plotted a colour magnitude diagram of the candidate clusters in this region:

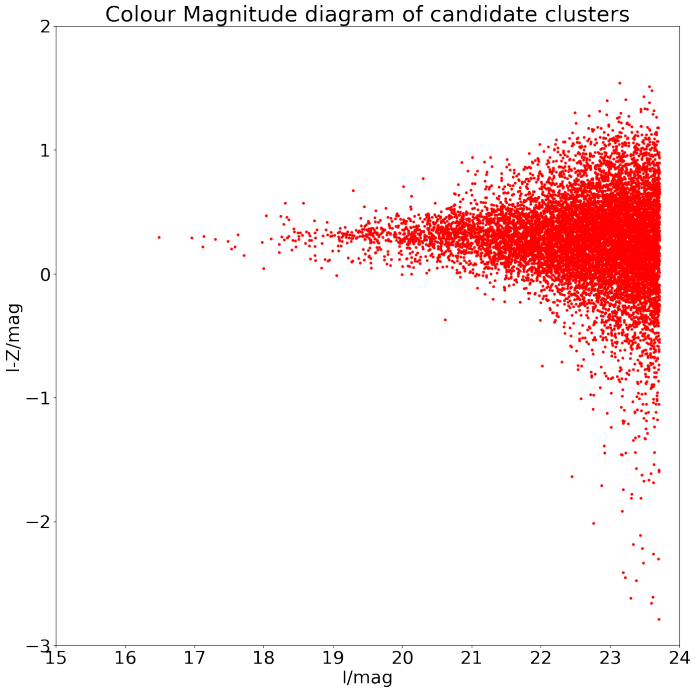

Figure 13: Plot of colour magnitude diagram for the galaxies within the 60 candidate clusters cells detected in the $25\,\mathrm{deg}^2$ area of SPT-E we searched.

Figure 13 has far more points than the similar plot in figure 9, however these candidate clusters have far more brighter galaxies too, which shows the red sequence in better resolution. Because there are significantly more points, the colour standard deviation is far closer to the fields colour standard deviation when compared to the same stats from the El Gordo cluster. These clusters have a colour standard deviation of 0.36, and the SPT-E field has a colour standard deviation of 0.37. This is far smaller than the difference of 0.1 found from the El Gordo region. The main cause of this is likely from a higher amount of galaxies in the galaxy cluster cells which may not be a part of the galaxy cluster itself, these galaxies are more likely to be a different colour than a cluster within the same cell. Additionally, each galaxy cluster will not be the same colour, which will increase the variance of colour compared to the variance of a singular cluster.

4 Discussion

RedMaPPer is an advanced galaxy cluster detection algorithm designed specifically to handle large photometric datasets such as the DES. It utilises colour data as part of the algorithm rather than as a qualitative review process as we have done. A catalogue of approximately 25,000 clusters was created by running redMaPPer on SDSS DR8.[11] We compared our data to this catalogue created using redMaPPer by considering a matching criteria: If our candidate clusters are within a square of side length 0.1125° centered on a redMaPPer cluster they are classified as a matched candidate. We also calculated the center points of our candidate clusters for this comparison. Plotting the location of our identified galaxy clusters with redMaPPer candidates within the same region of sky we get this graph:

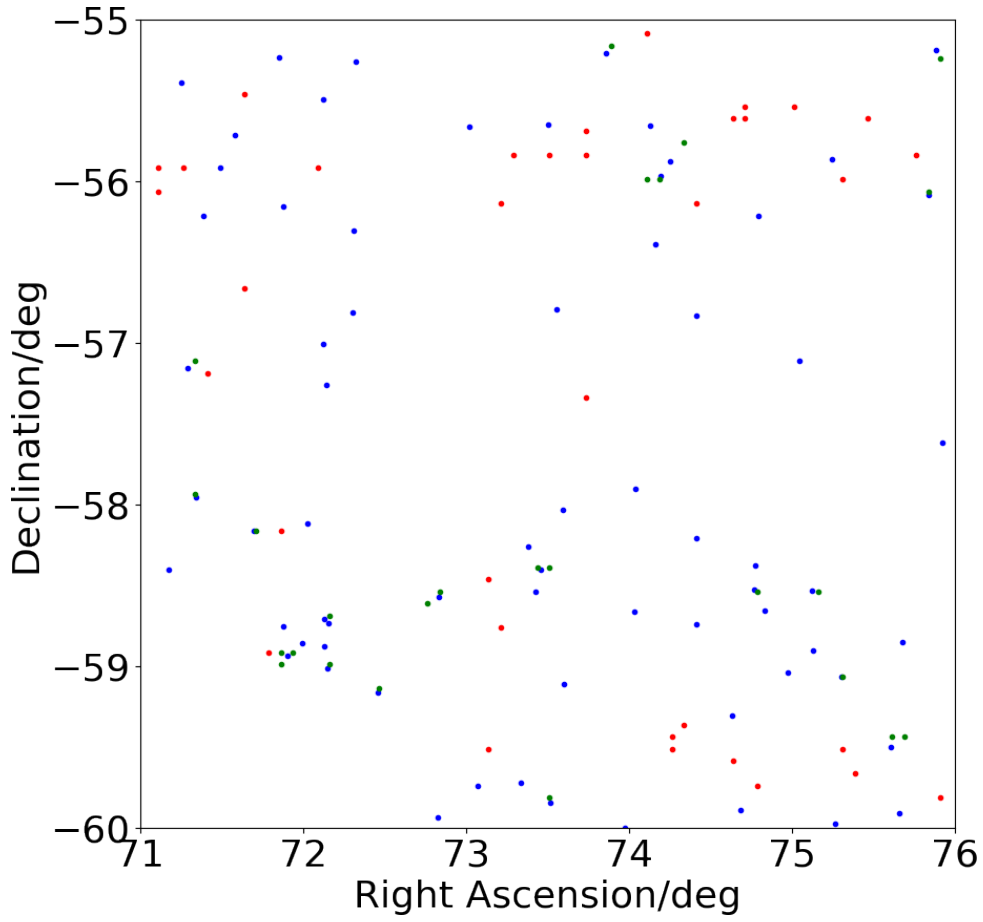

Figure 14: A plot of candidate clusters from the redMaPPer catalogue and our candidate clusters. Blue: redMaPPer candidate clusters Green: Our candidate clusters that meet the matching criteria. Red: Our candidate clusters that do not meet the matching criteria.

There are 68 clusters identified by redMaPPer within this SPT-E region which is a similar number to the candidate clusters we identified (60) which indicates that we have detected a reasonable density of galaxy clusters. Figure 14 has the whole spectrum of matching accuracy that you might expect: Candidates that matched correctly and agree with redMaPPer data, candidates that do not match but are near redMaPPer clusters and other candidates that meet the matching criteria, candidates that do not match but are in a region of high redMaPPer

cluster density, and candidates that are not near any other candidates or redMaPPer clusters. The ratio of our matched candidates vs unmatched candidates is $\frac{5}{12} \approx 0.42$. This may be due to the fact that the region we used to calculate the field standard deviation (σ_{field}) was far more uniform than the rest of the region; inflating the cell significance higher than the true value. This is one of the main issues with the counts in cells algorithm. Because counts in cells is simple it assumes the input of a flawless dataset. During the project we spent far more time than expected preparing the DES data to ensure that counts in cells didn't give us junk results, unfortunately this meant we weren't able to test a second detection algorithm due to time constrains. Some of the other issues with the counts in cells algorithm comes from dividing the field into cells. Some clusters may be undetected if they are split between multiple cells. This could be remedied by repeating the algorithm many times with small offsets. However creating a method of merging clusters found in overlaying cells may be more time consuming and computationally expensive than using a different algorithm entirely, such as a percolation algorithm instead. A major improvement for any algorithm to have over counts in cells, is to use colour data as part of the cluster identification process as opposed to using colour data to inspect the resulting candidate clusters.

In summary, the counts in cells algorithm is an imprecise method of detecting galaxy clusters at a broad range of redshifts: from z=0.25 to z=0.87. We detected 60 galaxy clusters in a $25\,\mathrm{deg}^2$ region of sky between $(73.5°, -58°)$ and $(75°, -56.5°)$ [format of(RA,DEC)]. Which compared to 68 clusters, detected in the same region of sky from literature. 42% of the candidate clusters we identified successfully matched with a candidate cluster from literature. This occurs if they are within 1.5 times the cell width of each other in either RA or DEC. The counts in cells algorithm suffers from an assumption of flawless supplied data which made it susceptible to identifying false positives for the region of sky we searched. The galaxy clusters identified showed a red sequence shown in figures 9 and 13. The counts in cells algorithm succeeds in detecting the largest, most significant galaxy clusters but struggles with smaller clusters. With the resources of modern computing at widespread disposal it's recommend more modern algorithm which uses colour data more proactively to be used instead of monochromatic searching algorithms.

Appendices

A Python scripts and output data

All python scripts and the candidate output file can be found on github:
`https://github.com/quasur/GaBSe`

References

[1] Oct 2012. URL `https://chandra.harvard.edu/xray_sources/galaxy_clusters.html`.

[2] Ehlert Steven. *The Co-evolution of Galaxies and Their Surrounding Environments in Massive Galaxy Clusters*. PhD thesis, Stanford University ProQuest Dissertations Publishing, 2013.

[3] Neta A. Bahcall. Large-scale structure in the universe indicated by galaxy clusters. *Annual Review of Astronomy and Astrophysics*, 26(1):631–686, 1988. doi:10.1146/annurev.aa.26.090188.003215.

[4] The Dark Energy Survey Collaboration. The dark energy survey: More than dark energy – an overview. *Monthly Notices of the Royal Astronomical Society*, 460(2):1270–1299, 2016. doi:10.1093/mnras/stw641.

[5] George O. Abell. The distribution of rich clusters of galaxies. *The Astrophysical Journal Supplement Series*, 3:211, 1958. doi:10.1086/190036.

[6] C R Nave. Stellar lifetimes, 2016. URL `http://hyperphysics.phy-astr.gsu.edu/hbase/Astro/startime.html`.

[7] Ryan Foltz. The red sequence method for galaxy cluster detection, Nov 2016. URL `https://astrobites.org/2012/03/27/the-red-sequence-method-for-galaxy-cluster-detection/`.

[8] David W. Hogg. Distance measures in cosmology, 2000.

[9] Planck Collaboration. Planck 2018 results. *Astronomy & Astrophysics*, 641:A6, sep 2020. doi:10.1051/0004-6361/201833910. URL `https://doi.org/10.1051%2F0004-6361%2F201833910`.

[10] Roy R. Gal. Optical detection of galaxy clusters, 2006.

[11] E. S. Rykoff, E. Rozo, M. T. Busha, C. E. Cunha, A. Finoguenov, A. Evrard, J. Hao, B. P. Koester, A. Leauthaud, B. Nord, and et al. Redmapper. i. algorithm and sdss dr8 catalog. *The Astrophysical Journal*, 785(2):104, 2014. doi:10.1088/0004-637x/785/2/104.

[12] S. Bocquet, J. P. Dietrich, T. Schrabback, L. E. Bleem, M. Klein, S. W. Allen, D. E. Applegate, M. L. Ashby, M. Bautz, M. Bayliss, and et al. Cluster cosmology constraints from the 2500 deg2 spt-sz survey: Inclusion of weak gravitational lensing data from magellan and the hubble space telescope. *The Astrophysical Journal*, 878(1):55, 2019. doi:10.3847/1538-4357/ab1f10.